Energy Partitioning Analysis of the Bonding in $L_2TM-C_2H_2$ and $L_2TM-C_2H_4$ (TM = Ni, Pd, Pt; L_2 = $(PH_3)_2$, $(PMe_3)_2$, $H_2PCH_2PH_2$, $H_2P(CH_2)_2PH_2$)†

Chiara Massera‡,§ and Gernot Frenking*,§

Dipartimento di Chimica Generale ed Inorganica, Chimica Analitica, Chimica Fisica, Università di Parma, Parco Area delle Scienze 17/A, 43100 Parma, Italy, and Fachbereich Chemie, Philipps-Universität Marburg, Hans-Meerwein-Strasse, D-35043 Marburg, Germany

Received March 6, 2003

The equilibrium geometries and bond dissociation energies of the complexes $L_2TM-C_2H_2$ and $L_2TM-C_2H_4$ (TM = Ni, Pd, Pt) with the monodentate ligands $L_2 = (PH_3)_2$, $(PMe_3)_2$ and the bidentate ligands $L_2 = \eta^2$-diphosphinomethane (dpm), η^2-diphosphinoethane (dpe) have been calculated using gradient-corrected DFT methods. The nature of the bonding interactions between the metal and the π ligands ethene and ethyne was investigated with an energy partitioning analysis (EPA). The ethene and ethyne ligands are more strongly bonded to the metal when L_2 = dpm, dpe. The EPA results reveal that the reason for the stronger bonds of (dpm)TM$-C_2H_x$ and (dpe)TM$-C_2H_x$ is the smaller preparation energy of (dpm)TM and (dpe)TM that is necessary to deform the metal fragments from the equilibrium geometry to the geometry in the complex. The $L_2TM-C_2H_x$ interaction energies between the fragments with a frozen geometry do not significantly vary when L_2 consists of a bidentate or two monodentate ligands. The EPA shows also that the nature of the $L_2TM-C_2H_x$ bonding does not change a lot when $L_2 = (PH_3)_2$, $(PMe_3)_2$ or when L_2 = dpm, dpe. The metal−carbon bonds always have a higher electrostatic (54.1−62.3%) than covalent (37.7−45.9%) character. The covalent bonding in the ethyne and ethene complexes comes mainly from the TM$\rightarrow C_2H_x$ in-plane π back-donation, while the relative contribution of the TM$\leftarrow C_2H_x$ σ donation is much less. The contributions of the out-of-plane $a_2(\delta)$ and $b_1(\pi_\perp)$ orbital interactions are very small even for the ethyne complexes. The bonding analysis suggests that the ethyne ligand in the complexes $(PH_3)_2TM-C_2H_2$ and $(PMe_3)_2TM-C_2H_2$ should be considered as a two-electron donor and not a four-electron donor.

Introduction

In 1951, Dewar introduced the molecular orbital model to describe the bonding of an ethene coordinated to Ag(I) or Cu(I).[1] Chatt and Duncanson[2] used Dewar's model for a systematic description of metal−ethene complexes. It is therefore nowadays called the DCD model after Dewar, Chatt, and Duncanson.[3] The DCD model has become the most important bonding model in transition metal (TM) chemistry not only for ethene complexes. The model suggests a synergistic TM←ligand σ donation from the occupied π orbital[4] of the ethene to the empty d(σ) orbitals of the metal, and a TM ligand π back-donation from the occupied d(π) AO of the metal to the empty π* orbital of the ligand. An alternative bonding model that is important for transition metals in high oxidation states has two electron-sharing σ bonds between the metal and the carbon atoms, which leads to a description of the molecule as a metallacyclopropane.[5,6] The two descriptions can be used for both alkene and alkyne complexes, the major difference between the two classes of compounds being the presence of a second $\pi_\perp$ orbital in alkynes, which is perpendicular to the TMC_2 plane, and which can be involved in the metal−ligand interactions. Due to this orbital, alkynes can be two- or four-electron donors. We will discuss the orbital interaction model in more detail below.

In this paper we report the results of quantum chemical calculations of alkene and alkyne complexes of the group 10 elements nickel, palladium, and platinum. Numerous theoretical studies of this class of compounds have been published in the last 20 years, focusing mainly on geometries and binding energies.[3b,6−17] The nature of the metal−ligand interactions was also analyzed by several workers. The discussion of the bonding situation was in most cases done in terms of the DCD model; that is, only the orbital interactions

* Corresponding author. E-mail: frenking@chemie.uni-marburg.de.

† Theoretical Studies of Organometallic Compounds. 49. Part 48: Rayón, V. M.; Frenking, G. *Organometallics*, in press.

‡ Università di Parma.

§ Universität Marburg.

(1) Dewar, M. J. S. *Bull. Soc. Chim. Fr.* **1951**, *18*, C79.

(2) Chatt, J.; Duncanson, L. A. *J. Chem. Soc.* **1953**, 2339.

(3) For a recent examination of the DCD model with modern quantum chemical methods see: (a) Frenking, G. J. *Organomet. Chem.* **2001**, *635*, 9. (b) Frenking G. *Modern Coordination Chemistry: The Legacy of Joseph Chatt*; Leigh, G. J., Winterton, N., Eds.; The Royal Society: London, 2002; p 111.

(4) The π symmetry assignment of the donor orbital of the ligand refers to the symmetry of the free ethene. In the complex, the π orbital of the free ethene has σ symmetry.

(5) (a) Pidun, U.; Frenking, G. *J. Organomet. Chem.* **1996**, *525*, 269. (b) Pidun, U.; Frenking, G. *J. Chem. Soc., Dalton Trans.* **1997**, 1653.

(6) Frenking, G.; Fröhlich, *N. Chem. Rev.* **2000**, *100*, 717.

10.1021/om0301637 CCC: $25.00
Publication on Web 05/29/2003

were considered. However, electrostatic attraction should also play an important role for the metal−ligand bonding in ethene complexes. Besides the attractive orbital and electrostatic interactions, there is strong Pauli repulsion between the ethene ligand and the metal fragment, which is important in order to give a physically meaningful insight into the nature of the bond.

A theoretical method that gives a quantitative estimate of the attractive orbital and electrostatic interactions as well as an estimate of the Pauli repulsion was introduced already in the 1970s independently by Morokuma[18] and by Ziegler.[19] Both workers used their methods for analyzing the bonding situation in alkene and alkyne complexes of group 10 elements.[7−9,12] The work by Morokuma et al.[8] was carried out only at the Hartree−Fock level. Therefore, a comparison with the present results is not appropriate. In the theoretical studies of Ziegler et al.[7,9,12] the authors used a questionable division of the interaction energy between the metal fragment and the ligand where the electrostatic attraction and the Pauli repulsion are added to give a term called steric energy. This has been criticized, because the steric term has no physical meaning and it has nothing to do with the loosely defined concept of steric interactions between substituents.[20] Because the electrostatic attraction and Pauli repulsion have opposite signs and often nearly cancel each other numerically, the addition of the two terms deceptively suggests that the metal−ligand bonding comes only from the orbital interactions. We suggest that the electrostatic attraction and Pauli repulsion have to be considered separately, so that the bonding contributions of the electrostatic and the orbital interactions can be properly compared to estimate the ratio of electrostatic and covalent bonding.

Two years ago we started a research program that aims at a quantitative analysis of the chemical bond in terms of electrostatic versus covalent interactions, also providing a estimate of the relative degree of multiple (π and δ) bonding of the covalent part, which is based on energy terms rather than partial charges. The program is based on the energy partitioning analyses of Morokuma[18] and Ziegler,[19] which are described in the Methods section. In previous studies we investigated the nature of the chemical bond in transition metal complexes with ligands CO,[21,22] with group-13 diyl ligands ER (E = B−Tl, R = Cp, $N(SiH_3)_2$, Ph, Me, NH_2, H),[22,23] with the ligands Cp and Ph,[24,25a] with the ligands cyc-E_5 (E = N−Sb) which are valence isoelectronic with Cp,[25] and with phosphane ligands PR_3 (R = H, Me, Cl, F).[26] We also investigated complexes with side-on and end-on coordinated ligands N_2, P_2, As_2, Sb_2, and Bi_2.[27] More recently we moved toward analyzing chemical bonds between main group elements. We studied main group metallocenes Cp_2E (E = Be−Ba, Zn, Si−Pb) and CpE (E = Li−Cs, B−Tl)[28] and phosphane complexes X_3B-PY_3 and X_3Al-PY_3 (X = H, F, Cl; Y = F, Cl, Me, CN).[29] Part of this work has been summarized in a review.[20]

We have now extended these studies to ethene and ethyne complexes of the complete triad of group 10 elements. Here we present our results of the bonding analysis of the complexes $L_2TM-C_2H_2$ and $L_2TM-C_2H_4$ (TM = Ni, Pd, Pt; L_2 = $(PH_3)_2$, $(PMe_3)_2$, dpm, dpe). The breakdown of the metal−ligand interaction energy into physically meaningful terms gives a comprehensive description of the nature of the bonding. The EPA results also settle the question whether the alkyne complexes $L_2TM-C_2H_2$ should be considered as 16-electron complexes or as 18-electron complexes, i.e., whether ethyne serves as a two-electron or four-electron donor in the molecules. A previous charge-partitioning analysis of $(PH_3)_2Ni-C_2H_2$ by Hyla-Krispin et al. revealed that ethyne serves as a four-electron donor in the compound, which should be considered an 18-electron complex.[17] It was later pointed out that the NBO data that are reported in this work are not in agreement with the assignment of an 18-electron complex and that an energy decomposition analysis should be carried out in order to address the question in an unbiased way.[30] This is now done in the context of the present study.

Methods

The geometries and bond dissociation energies have been calculated at the nonlocal DFT level of theory using the exchange functional of Becke[31] and the correlation functional of Perdew[32] (BP86). Scalar relativistic effects have been considered using the zero-order regular approximation (ZORA).[33,34] Uncontracted Slater-type orbitals (STOs) were used as basis functions for the SCF calculations.[35] The basis sets for all atoms have triple-ζ quality augmented with one set of polarization functions, i.e., p functions on hydrogen, d functions on carbon and phosphorus, and f functions on the

(7) Ziegler, T.; Rauk, A. *Inorg. Chem.* **1979**, *18*, 1558.
(8) Kitaura, K.; Sakaki, S.; Morokuma, K. *Inorg. Chem.* **1981**, *20*, 2292.
(9) Ziegler, T. *Inorg. Chem.* **1985**, *24*, 1547.
(10) Morokuma, K.; Borden, W. T. *J. Am. Chem. Soc.* **1991**, *113*, 1912.
(11) Sakaki, S.; Ieki, M. *Inorg. Chem.* **1991**, *30*, 4218.
(12) Li, J.; Schreckenbach, G.; Ziegler, T. *Inorg. Chem.* **1995**, *34*, 3245.
(13) Frenking, G.; Antes, I.; Böhme, M.; Dapprich, S.; Ehlers, A. W.; Jonas, V.; Neuhaus, A.; Otto, M.; Stegmann, R.; Veldkamp, A.; Vyboishchikov, S. F. In *Reviews in Computational Chemistry*; Lypkowitz, K. B., Boyd, D. B., Eds.; VCH Publishers: New York, 1996; Vol. 8, p 63.
(14) Uddin, J.; Dapprich, S.; Frenking, G.; Yates, B. F. *Organometallics* **1999**, *18*, 457.
(15) Yates, B. F. *J. Mol. Struct. (THEOCHEM)* **2000**, *506*, 223.
(16) Sakaki, S.; Yamaguchi, S.; Musashi, Y.; Sugimoto, M. *J. Organomet. Chem.* **2001**, *635*, 173.
(17) Hyla-Kryspin, I.; Koch, J.; Gleiter, R.; Klettke, T.; Walther, D. *Organometallics* **1998**, *17*, 4724.
(18) (a) Morokuma, K. *J. Chem. Phys.* **1971**, *55*, 1236. (b) Morokuma, K. *Acc. Chem. Res.* **1977**, *10*, 294.
(19) Ziegler, T.; Rauk, A. *Theor. Chim. Acta* **1977**, *46*, 1.
(20) Frenking, G.; Wichmann, K.; Fröhlich, N.; Loschen, C.; Lein, M.; Frunzke, J.; Rayón, V. M. *Coord. Chem. Rev.* **2003**, *238−239*, 55.
(21) Diefenbach, A.; Bickelhaupt F. M.; Frenking, G. *J. Am. Chem. Soc.* **2000**, *122*, 6449.
(22) (a) Chen, Y.; Frenking, G. *J. Chem. Soc., Dalton Trans.* **2001**, 434. (b) Doerr M.; Frenking, G. *Z. Allg. Anorg. Chem.* **2002**, *628*, 843.
(23) Uddin J.; Frenking, G. *J. Am. Chem. Soc.* **2001**, *123*, 1683.
(24) Rayón V. M.; Frenking, G. *Organometallics*, in press.
(25) (a) Lein, M.; Frunzke, J.; Timoshkin, A.; Frenking, G. *Chem. Eur. J.* **2001**, *7*, 4155. (b) Frunzke, J.; Lein, M.; Frenking, G. *Organometallics* **2002**, *21*, 3351.
(26) Frenking, G.; Wichmann, K.; Fröhlich, N.; Grobe,J.; Golla, W.; Le Van, D.; Krebs B.; Läge, M. *Organometallics* **2002**, *21*, 2921.
(27) Esterhuysen, C.; Frenking, G. *Chem. Eur. J.*, in press.
(28) Rayón, V. M.; Frenking, G. *Chem. Eur. J.* **2002**, *8*, 4693.
(29) Loschen, C.; Voigt, K.; Frunzke, J.; Diefenbach, A.; Diedenhofen, M.; Frenking, G. *Z. Allg. Anorg. Chem.* **2002**, *628*, 1294.
(30) Reference 6, page 756f.
(31) Becke, A. D. *Phys. Rev. A* **1988**, *38*, 3098.
(32) Perdew, J. P. *Phys. Rev. B* **1986**, *33*, 8822.
(33) Snijders, J. G. *Mol. Phys.* **1978**, *36*, 1789.
(34) Snijders, J. G.; Ros, P. *Mol. Phys.* **1979**, *38*, 1909.
(35) Snijders, J. G.; Baerends, E. J.; Vernooijs, P. *At. Nucl. Data Tables* **1982**, *26*, 483.

metals. The $(1s2s2p)^{10}$ core electrons of the transition metals and the $1s^2$ core electrons of carbon and phosphorus were treated by the frozen core approximation.[36] An auxiliary set of s, p, d, f, and g STOs was used to fit the molecular densities and to represent the Coulomb and exchange potentials accurately in each SCF cycle.[37] This level of theory is denoted BP86/TZP. The latter calculations were carried out with the program package ADF 2000.01.[38] The geometries have also been optimized with the program package Gaussian 98[39] using B3LYP[40] in conjunction with the LANL2DZ effective core potentials[41] for Ni, Pd, and Pt and 6-31G(d) basis sets for the other atoms.[42] This level of theory is denoted B3LYP/LANL2DZ*. The latter calculations were carried out because the vibrational frequencies at B3LYP/LANL2DZ* could be calculated using analytical second derivatives. All structures that are reported here are energy minima on the B3LYP/LANL2DZ* potential energy surface.

The nature of the metal−ethene and metal−ethyne bonding has been investigated through the energy-partitioning analysis (EPA) of the program package ADF based on the EDA method of Morokuma[18] and the ETS partitioning scheme of Ziegler.[19] The bonding analysis was carried out at the BP86/TZP level. In the EPA method the bond dissociation energy D_e between two fragments A and B is partitioned into several contributions which can be identified as physically meaningful entities. In the present case the fragments are L_2TM and C_2H_x in the singlet ground state. First, D_e is separated into two major components, ΔE_{prep} and ΔE_{int}:

$$-D_e = \Delta E_{prep} + \Delta E_{int} \quad (1)$$

ΔE_{prep} is the energy that is necessary to promote the fragments L_2TM and C_2H_x from their equilibrium geometry to the geometry that they have in the complex $L_2TM-C_2H_x$. ΔE_{int} is the instanteneous interaction energy between the two fragments in the molecule. Note that it is ΔE_{int} and not D_e that should be used to identify the nature of the chemical bond. The interaction energy ΔE_{int} can be divided into three components:

$$\Delta E_{int} = \Delta E_{elstat} + \Delta E_{Pauli} + \Delta E_{orb} \quad (2)$$

ΔE_{elstat} gives the electrostatic interaction energy between the fragments that are calculated with a frozen electron density distribution in the geometry of the complex. It can be considered as an estimate of the *electrostatic* contribution to the bonding interactions. The second term ΔE_{Pauli} in eq 1 gives the repulsive four-electron interactions between occupied orbitals. ΔE_{Pauli} is calculated by enforcing the Kohn−Sham determinant of the molecule which results from superimposing the fragments to be orthonormal through antisymmetrization and renormalization. The stabilizing orbital interaction term ΔE_{orb} is calculated in the final step of the analysis when the Kohn−Sham orbitals relax to their final form. The orbital term ΔE_{orb} can be considered as an estimate of the *covalent* contributions to the attractive interactions. Thus, the ratio $\Delta E_{elstat}/\Delta E_{orb}$ indicates the electrostatic/covalent character of the bond. The latter term can be partitioned further into contributions by the orbitals that belong to different irreducible representations of the interacting system. This makes it possible to calculate, for example, the contributions of σ and π bonding to a covalent multiple bond. More details about the method can be found in ref 38b.

Geometries and Bond Energies

Figure 1 shows schematically the optimized structures and the most important bond lengths and bond angles in the complexes. The complete sets of interatomic distances and angles are given as Supporting Information. Figure 1 also gives the theoretically predicted bond dissociation energies (BDEs) of the $L_2TM-C_2H_x$ bonds at BP86/TZP.

The calculated geometries and bond energies shall be discussed only shortly because the molecules have already been studied in previous theoretical investigations.[12−17] Our calculated bond lengths and angles are in good agreement with earlier works which report about geometries optimized at different level of theory. Figure 1 also gives for some complexes the experimental values of TM−C and C−C distances which have been reported for substituted analogues of the model compounds. The theoretically predicted TM−C bond lengths are always slightly longer than the experimental values. The difference can be explained with the influence of the substituents and with solid state effects. It has been shown that donor−acceptor bonds are shorter in the solid state than in the gas phase because of intermolecular interactions.[58] The differences between theoretical and experimental values in Figure 1 are not very large, however.

(36) Baerends, E. J.; Ellis, D. E.; Ros, P. *Chem. Phys.* **1973**, *2*, 41.
(37) Krijn, J.; Baerends, E. J. *Fit Functions in the HFS-Method*; Internal Report (in Dutch); Vrije Universiteit Amsterdam: The Netherlands, 1984.
(38) (a) Bickelhaupt, F. M.; Baerends, E. J. *Rev. Comput. Chem.* **2000**, *15*, 1. (b) te Velde, G.; Bickelhaupt, F. M.; Baerends, E. J.; van Gisbergen, S. J. A.; Fonseca Guerra, C.; Snijders, J. G.; Ziegler, T. *J. Comput. Chem.* **2001**, *22*, 931.
(39) Frisch, M. J.; Trucks, G. W.; Schlegel, H. B.; Scuseria, G. E.; Robb, M. A.; Cheeseman, J. R.; Zakrzewski, V. G.; Montgomery, Jr., J. A.; Stratmann, R. E.; Burant, J. C.; Dapprich, S.; Millam, J. M.; Daniels, A. D.; Kudin, K. N.; Strain, M. C.; Farkas, O.; Tomasi, J.; Barone, V.; Cossi, M.; Cammi, R.; Mennucci, B.; Pomelli, C.; Adamo, C.; Clifford, S.; Ochterski, J.; Petersson, G. A.; Ayala, P. Y.; Cui, Q.; Morokuma, K.; Malick, D. K.; Rabuck, A. D.; Raghavachari, K.; Foresman, J. B.; Cioslowski, J.; Ortiz, J. V.; Stefanov, B. B.; Liu, G.; Liashenko, A.; Piskorz, P.; Komaromi, I.; Gomperts, R.; Martin, R. L.; Fox, D. J.; Keith, T.; Al-Laham, M. A.; Peng, C. Y.; Nanayakkara, A.; Gonzalez, C.; Challacombe, M.; Gill, P. M. W.; Johnson, B.; Chen, W.; Wong, M. W.; Andres, J. L.; Gonzalez, C.; Head-Gordon, M.; Replogle, E. S.; Pople, J. A. *Gaussian 98*, Revision A.3; Gaussian, Inc.: Pittsburgh, PA, 1998.
(40) (a) Becke, A. D. *J. Chem. Phys.* **1993**, *98*, 5648. (b) Lee, C.; Yang, W.; Parr, R. G. *Phys. Rev. B* **1988**, *37*, 785.
(41) Hay, P. J.; Wadt, W. R. *J. Chem. Phys.* **1985**, *82*, 299.
(42) (a) Ditchfield, R.; Hehre, W. J.; Pople, J. A. *J. Chem. Phys.* **1971**, *54*, 724. (b) Hehre, W. J.; Ditchfield, R.; Pople, J. A. *J. Chem. Phys.* **1972**, *56*, 2257.
(43) Dreissig, W.; Dietrich, H. *Acta Crystallogr., Sect. B* **1981**, *37*, 931.
(44) Pörsche, R.; Tsay, Y.-H.; Krüger, C. *Angew. Chem., Int. Ed. Engl.* **1985**, *24*, 323.
(45) Okamoto, K.; Kai, G.; Yasuoka, N.; Kasai, N. *J. Organomet. Chem.* **1974**, *65*, 427.
(46) Farrar, H.; Payne N. C. *J. Organomet. Chem.* **1981**, *220*, 239.
(47) Cheng, P.-T.; Nyburg, S. C. *Can. J. Chem.* **1972**, *50*, 912.
(48) Davies, B. W.; Payne, N. C. *J. Organomet. Chem.* **1975**, *99*, 315.
(49) Packett, D. L.; Syed, A.; Trogler, W. C. *Organometallics* **1988**, *7*, 159.
(50) Hofmann, P.; Perez-Moya, L. A.; Krause, M. E.; Kumberger, O.; Muller, G. *Z. Naturforsch., Teil B* **1990**, *45*, 897.
(51) Ficker, R.; Hiller, W.; Regius, C. T.; Hofmann, P. *Z. Kristallogr.*, **1996**, *211*, 58.
(52) Bach, I.; Porsche, K.-R.; Proft, B.; Goddard, R.; Kopiske, C.; Krüger, C.; Rufinska, A.; Seevogel, K. *J. Am. Chem. Soc.* **1997**, *119*, 3773.
(53) Porsche, K. R.; Mynott, R.; Angermund, K.; Kruger, C. *Z. Naturforsch. Teil B* **1985**, *40*, 199.
(54) Benn, R.; Betz, P.; Goddard, R.; Jolly, P. W.; Kokel, N.; Krüger, C.; Topalovic, I. *Z. Naturforsch., Teil B* **1991**, *46*, 1395.
(55) Schager, F.; Bonrath, W.; Pörschke, K.-R.; Kessler, M.; Krüger, C.; Seevogel, K. *Organometallics* **1997**, *16*, 4276.
(56) Wicht, D. K., Zhuravel, M. A.; Gregush, R. V.; Glueck, D. S.; Guzei, I. A.; Liable-Sands, L. M.; Rheingold, A. L. *Organometallics* **1998**, *17*, 1412.
(57) Muller, C.; Lachicotte, R.J.; Jones, W. D. *Organometallics* **2002**, *21*, 1118.
(58) Jonas, V.; Frenking, G.; Reetz, M. T. *J. Am. Chem. Soc.* **1994**, *116*, 8741.

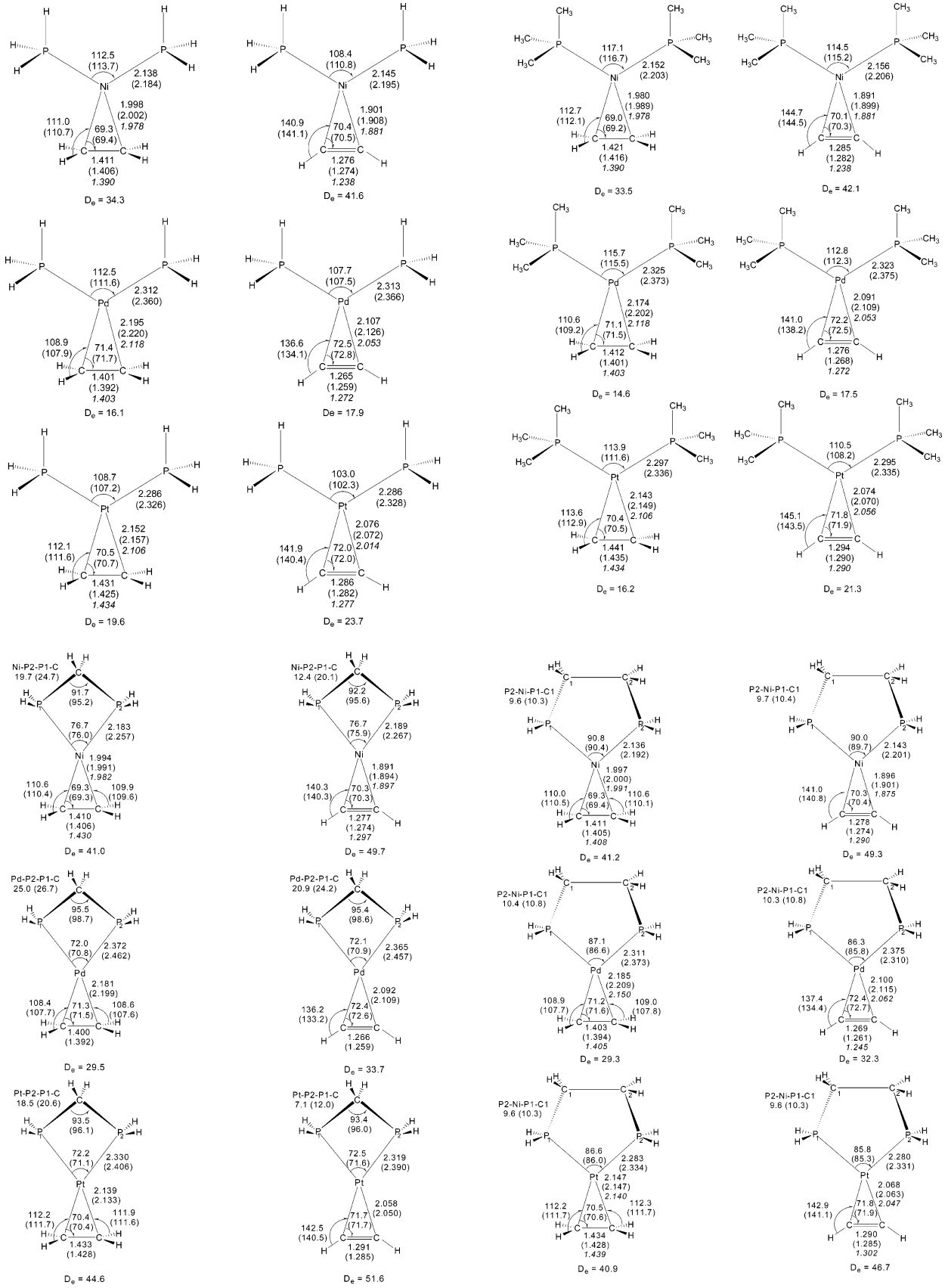

Figure 1. Calculated bond lengths [Å] and angles [deg] and theoretically predicted bond dissociation energies of the π ligands [kcal/mol] of $L_2TM-C_2H_x$ at BP86/TZP (B3LYP/LANL2DZ*). Experimental bond lengths of substituted analogues are given *in italics*. The experimental values have been taken from the following complexes: $(Ph_3P)_2Ni(C_2H_4)$,[43] $(Ph_3P)_2Ni(C_2H_2)$,[44] $(Ph_3P)_2Pd(CH_2CCH_2)$,[45] $[(C_6H_{11})_3P]_2Pd(CF_3CCCF_3)$,[46] $(Ph_3P)_2Pt(C_2H_4)$,[47] $(Ph_3P)_2Pt(H_3CCCPh)$,[48] $(Me_3P)_2Pt(PhCCPh)$,[49] $[(tBu)_2P(CH_2)P(tBu)_2]Ni[Ph(CH)_2Ph]$,[50] $[(tBu)_2P(CH_2)P(tBu)_2]Ni[Me_3SiCCSiMe_3]$,[51] $[(^iPr)_2P(CH_2)_2(^iPr)_2P]Ni(C_8H_8)$,[52] $[Me_2P(CH_2)_2PMe_2]Ni(PhCCPh)$,[53] $[(C_6H_{11})_2P(CH_2)_2P(C_6H_{11})_2]Pd(CH_2CHCHCH_2)$,[54] $[(^iPr)_2P(CH_2)_2P(^iPr)_2]Pd(HCCPh)$,[55] $[Ph_2P(MeCH)_2PPh_2]Pt(PhCHCHPh)$,[56] $[(^iPr)_2P(CH_2)_2P(^iPr)_2]Pt(PhCCPh)$.[57]

Table 1. Energy Decomposition Analysis of $(PH_3)_2TM-C_2H_x$ at BP86/TZP (kcal/mol)

	Ni(PH$_3$)$_2$		Pd(PH$_3$)$_2$		Pt(PH$_3$)$_2$	
	C_2H_4	C_2H_2	C_2H_4	C_2H_2	C_2H_4	C_2H_2
$\Delta E(=-D_e)$	−34.3	−41.5	−16.1	−17.9	−19.6	−23.7
ΔE_{prep}(tot)	20.4	30.8	20.9	30.9	39.3	51.3
$\Delta E_{prep}(C_2H_x)$	9.2	18.1	7.2	15.2	12.8	21.4
$\Delta E_{prep}(L_2TM)$	11.2	12.7	13.7	15.7	26.5	29.9
ΔE_{int}	−54.6	−72.3	−37.0	−48.8	−58.9	−75.0
ΔE_{Pauli}	143.4	167.5	138.1	162.0	205.7	228.8
ΔE_{elstat}[a]	−114.4 (57.8%)	−132.2 (55.1%)	−109.1 (62.3%)	−125.6 (59.6%)	−159.8 (60.4%)	−174.7 (57.5%)
ΔE_{orb}[a]	−83.6 (42.2%)	−107.6 (44.9%)	−66.0 (37.7%)	−85.2 (40.4%)	−104.8 (39.6%)	−129.1 (42.5%)
$\Delta E(a_1)_\sigma$[b]	−21.1 (25.2%)	−21.7 (20.2%)	−20.3 (30.8%)	−22.0 (25.8%)	−36.1 (34.4%)	−38.1 (29.5%)
$\Delta E(a_2)_\delta$[b]	−0.2 (0.3%)	−3.5 (3.1%)	−0.3 (0.4%)	−1.7 (2.1%)	−0.7 (0.7%)	−3.0 (2.3%)
$\Delta E(b_1)\pi_\perp$[b]	−3.4 (4.0%)	−5.5 (5.1%)	−2.9 (4.4%)	−4.1 (4.8%)	−4.6 (4.4%)	−6.5 (5.1%)
$\Delta E(b_2)\pi_\parallel$[b]	−58.9 (70.5%)	−77.0 (71.6%)	−42.5 (64.4%)	−57.3 (67.3%)	−63.4 (60.5%)	−81.5 (63.1%)

[a] Values in parentheses give the percentage of attractive interactions $\Delta E_{elstat} + \Delta E_{orb}$. [b] Values in parentheses gives the percentage contribution to the total orbital interactions.

The most relevant data given in Table 1 that are important for this work are the bond dissociation energies. The calculations predict that the BDE values of the complexes with the monodentate phosphane ligands $(PH_3)_2TM-C_2H_x$ and $(PMe_3)_2TM-C_2H_x$ have a trend for the different metals of TM Ni ≫ Pt > Pd. The ethyne ligand is always more strongly bound than the ethene one. This could be interpreted as support of ethyne serving as a four-electron donor. The analysis of the metal−ligand interactions given below will address this point. We want to point out that the complexes $(PMe_3)_2TM-C_2H_x$ have slightly *lower* BDE values than the respective $(PH_3)_2TM-C_2H_x$ species except for the ethyne complexes of nickel, where the D_e values are nearly the same (Figure 1). A speculative interpretation would suggest that, with comparison to PH_3, the PMe_3 ligand weakens the $TM-C_2H_x$ bonding interactions. It will be seen below if this interpretation is justified.

The calculated bond dissociation energies of the complexes with the bidentate phosphane ligands (dpm)-$TM-C_2H_x$ and (dpe)$TM-C_2H_x$ are very interesting. The BDE values of the latter complexes are always significantly higher than those of the complexes with monodentate phosphane ligands. The bidentate ligands not only yield larger bond energies but also change the trend of the BDE values for the different metals. Figure 1 shows that the bond dissociation energies of (dpm)$TM-C_2H_x$ display the order Pt > Ni ≫ Pd; that is, the platinum complexes are now the strongest bonded species. The BDEs of the platinum complexes (dpe)$Pt-C_2H_x$ are also rather large, but the nickel complexes (dpe)$Ni-C_2H_x$ remain the strongest bonded molecules of the series (dpe)$TM-C_2H_x$, which, therefore, has the order Ni > Pt ≫ Pd.

We want to draw attention to the finding that the calculated C−C distances in the complexes do not agree with the trend of the theoretically predicted $L_2TM-C_2H_x$ bond dissociation energies. The carbon−carbon bonds in the complexes are always longer than in the free ligands. The calculated C−C distances at BP86/TZP of ethene and ethyne are 1.332 and 1.205 Å, respectively. Figure 1 shows that the compounds $(PMe_3)_2Pt-C_2H_x$ have the most stretched carbon−carbon bond lengths among the platinum complexes $L_2Pt-C_2H_x$, but the bond dissociation energies of $(PMe_3)_2Pt-C_2H_2$ (D_e = 21.3 kcal/mol) and $(PMe_3)_2Pt-C_2H_4$ (D_e = 16.2 kcal/mol) are the lowest BDE values in the series. The calculated data indicate clearly that *there is no correlation between the metal−ligand bond energies and the geometries of the molecules*. This is an important result because it is often assumed that the observed bond lengths and bond angles are a probe for the bond strength. The results of the energy partitioning analysis, which shall be presented and discussed below, will give an explanation for the above findings.

Bonding Analysis

The EPA results of the complexes $L_2TM-C_2H_x$ with four different ligands L_2 are given in Tables 1−4. The three top entries give the values of the dissociation energy D_e, the preparation energy ΔE_{prep}, and the interaction energy ΔE_{int}. The calculated data show that the complexes with monodentate phosphane ligands $(PH_3)_2TM-C_2H_x$ and $(PMe_3)_2TM-C_2H_x$ have much larger preparation energies than the complexes with bidentate phosphane ligands (dpm)$TM-C_2H_x$ and (dpe)$TM-C_2H_x$. The breakdown of the ΔE_{prep} values into contributions of the metal fragments L_2TM and the π ligand C_2H_x shows that the former species are responsible for the larger preparation energy of $(PH_3)_2TM-C_2H_x$ and $(PMe_3)_2TM-C_2H_x$. This is because the equilibrium structures of free $(PH_3)_2TM$ and $(PMe_3)_2TM$ present a linear arrangement of the ligands; that is, the bond angle P−TM−P′ is 180°. The latter angle becomes much more acute in the complexes where the bond angle P−TM−P′ is between 103° and 117.1° (Figure 1).

The larger preparation energies of $(PH_3)_2TM-C_2H_x$ and $(PMe_3)_2TM-C_2H_x$ are the reason the dissociation energies D_e of the complexes are rather small. Tables 1−4 show that the interaction energies of $(PH_3)_2TM-C_2H_x$ and $(PMe_3)_2TM-C_2H_x$ are nearly as high or even higher than the ΔE_{int} values of (dpm)$TM-C_2H_x$ and (dpe)$TM-C_2H_x$. A striking example is given by the energy values of $(PMe_3)_2Pt-C_2H_2$ and (dpm)$Pt-C_2H_2$. The dissociation energy of the latter complex (D_e = 51.6 kcal/mol) is much higher than for the former complex (D_e = 21.3 kcal/mol), but the metal−ligand interaction energy of $(PMe_3)_2Pt-C_2H_2$ (ΔE_{int} = −80.3 kcal/mol) is nearly the same as that of (dpm)$Pt-C_2H_2$ (ΔE_{int} = −81.7 kcal/mol). The interaction energies of the latter two molecules represent also two of the largest values that have been calculated for the ethyne complexes (Tables 1−4) which is in agreement with the rather long C−C distances of the compounds (Figure 1). Thus, the ΔE_{int} values are a better probe to estimate the strength of

Table 2. Energy Decomposition Analysis of $(PMe_3)_2TM-C_2H_x$ at BP86/TZP (kcal/mol)

	$Ni(PMe_3)_2$		$Pd(PMe_3)_2$		$Pt(PMe_3)_2$	
	C_2H_4	C_2H_2	C_2H_4	C_2H_2	C_2H_4	C_2H_2
$\Delta E(=-D_e)$	−33.5	−42.1	−14.6	−17.5	−16.2	−21.3
ΔE_{prep}(tot)	26.5	38.6	26.6	39.2	45.8	59.0
$\Delta E_{prep}(C_2H_x)$	11.8	22.2	9.5	19.7	15.6	25.3
$\Delta E_{prep}(L_2TM)$	14.7	16.4	17.1	19.5	30.2	33.7
ΔE_{int}	−60.0	−80.7	−41.2	−56.7	−62.0	−80.3
ΔE_{Pauli}	166.0	186.0	157.7	179.6	226.9	244.9
ΔE_{elstat}[a]	−128.9 (57.0%)	−144.3 (54.1%)	−122.5 (61.6%)	−137.7 (58.3%)	−173.5 (60.1%)	−184.9 (56.9%)
ΔE_{orb}[a]	−97.1 (43.0%)	−122.4 (45.9%)	−76.4 (38.4%)	−98.6 (41.7%)	−115.4 (39.9%)	−140.3 (43.1%)
$\Delta E(a_1)_\sigma$[b]	−21.2 (21.8%)	−22.3 (18.2%)	−20.5 (26.8%)	−22.8 (23.1%)	−35.8 (31.0%)	−38.4 (27.4%)
$\Delta E(a_2)_\delta$[b]	−0.2 (0.3%)	−4.0 (3.3%)	−0.3 (0.4%)	−2.0 (2.1%)	−0.7 (0.7%)	−3.3 (2.3%)
$\Delta E(b_1)\pi_\perp$[b]	−4.0 (4.1%)	−5.3 (4.3%)	−3.3 (4.3%)	−4.2 (4.2%)	−5.0 (4.3%)	−6.1 (4.4%)
$\Delta E(b_2)\pi_\parallel$[b]	−71.7 (73.8%)	−90.8 (74.2%)	−52.3 (68.5%)	−69.6 (70.6%)	−73.9 (64.0%)	−92.5 (65.9%)

[a] Values in parentheses give the percentage of attractive interactions $\Delta E_{elstat} + \Delta E_{orb}$. [b] Values in parentheses gives the percentage contribution to the total orbital interactions.

Table 3. Energy Decomposition Analysis of $(dpm)TM-C_2H_x$ at BP86/TZP (kcal/mol)

	Ni(dpm)		Pd(dpm)		Pt(dpm)	
	C_2H_4	C_2H_2	C_2H_4	C_2H_2	C_2H_4	C_2H_2
$\Delta E(=-D_e)$	−41.0	−49.7	−29.5	−33.7	−44.6	−51.6
ΔE_{prep}(tot)	14.1	24.2	10.4	17.8	20.0	29.7
$\Delta E_{prep}(C_2H_x)$	8.3	17.6	6.8	14.8	12.9	22.4
$\Delta E_{prep}(L_2TM)$	5.8	6.6	3.6	3.0	7.1	7.3
ΔE_{int}	−55.1	−73.9	−40.0	−51.5	−64.6	−81.3
ΔE_{Pauli}	136.2	168.2	132.6	160.9	200.8	233.7
ΔE_{elstat}[a]	−109.8 (57.4%)	−132.6 (54.8%)	−107.0 (62.0%)	−126.1 (59.4%)	−159.0 (59.9%)	−179.7 (57.1%)
ΔE_{orb}[a]	−81.5 (42.6%)	−109.5 (45.2%)	−65.6 (38.0%)	−86.3 (40.6%)	−106.4 (40.1%)	−135.3 (42.9%)
$\Delta E(a')$[b]	−22.7 (27.9%)	−26.7 (24.4%)	−21.4 (32.6%)	−24.9 (28.9%)	−39.0 (36.7%)	−44.6 (33.0%)
$\Delta E(a'')$[b]	−58.8 (72.1%)	−82.8 (75.6%)	−44.2 (67.4%)	−61.4 (71.1%)	−67.4 (63.3%)	−90.7 (67.0%)

[a] Values in parentheses give the percentage of attractive interactions $\Delta E_{elstat} + \Delta E_{orb}$. [b] Values in parentheses gives the percentage contribution to the total orbital interactions.

Table 4. Energy Decomposition Analysis of $(dpe)TM-C_2H_x$ at BP86/TZP (kcal/mol)

	Ni(dpe)		Pd(dpe)		Pt(dpe)	
	C_2H_4	C_2H_2	C_2H_4	C_2H_2	C_2H_4	C_2H_2
$\Delta E(=-D_e)$	-41.2	-49.3	-29.3	-32.3	-41.0	-46.7
ΔE_{prep}(tot)	14.9	25.6	11.8	21.6	23.9	35.0
$\Delta E_{prep}(C_2H_x)$	8.7	18.3	7.3	16.0	13.2	22.7
$\Delta E_{prep}(L_2TM)$	6.2	7.3	4.5	5.6	10.7	12.3
ΔE_{int}	−56.1	−74.9	−41.1	−53.9	−64.9	−81.7
ΔE_{Pauli}	133.4	161.0	132.8	159.0	196.8	224.4
ΔE_{elstat}[a]	−108.3 (57.2%)	−128.2 (54.4%)	−107.1 (61.6%)	−125.0 (58.7%)	−156.0 (59.6%)	−173.3 (56.6%)
ΔE_{orb}[a]	−81.2 (42.8%)	−107.7 (45.6%)	−66.8 (38.4%)	−87.9 (41.3%)	−105.7 (40.4%)	−132.8 (43.4%)
$\Delta E(a)$[b]	−19.3 (23.8%)	−23.7 (22.0%)	−18.8 (28.1%)	−22.5 (25.6%)	−34.5 (32.6%)	−39.6 (29.8%)
$\Delta E(b)$[b]	−61.9 (76.2%)	−84.0 (78.0%)	−48.0 (71.9%)	−65.4 (74.4%)	−71.2 (67.4%)	−93.2 (70.2%)

[a] Values in parentheses give the percentage of attractive interactions $\Delta E_{elstat} + \Delta E_{orb}$. [b] Values in parentheses gives the percentage contribution to the total orbital interactions.

the metal−ligand interactions than the D_e values. The interaction energies can be further partitioned into the three difference contributions, which were described above.

Tables 1−4 show that the largest contributions to the $L_2TM-C_2H_x$ interactions come from the repulsive term ΔE_{Pauli}. The ratio of the attractive contributions ΔE_{elstat} and ΔE_{orb} gives an estimate of the electrostatic and covalent character of the bond. The results in Table 4 show that the percentage values of ΔE_{elstat} and ΔE_{orb} in $L_2TM-C_2H_x$ change very little for different phosphane ligands L_2. The electrostatic contribution is always larger than the covalent contribution to the bonding interaction; that is, the character of the $L_2TM-C_2H_x$ bonds is more electrostatic than covalent. The ΔE_{elstat} term yields between 54.1 and 62.3% of the attractive interactions. The metal−carbon bonding in the ethyne complexes has a slightly higher covalent character than in the ethene complexes. The covalent character increases for different metals TM with Pd < Pt < Ni. The EPA makes it possible to identify the type of orbitals that are important for the covalent bonding.

Figure 2 shows a qualitative orbital interaction diagram between a transition metal and a π ligand, which illustrates the DCD bonding model for ethene and alkyne complexes. There are four principle bonding components for the latter species and two components for the former complexes. The in-plane orbitals which yield metal←ligand donation have σ symmetry[4] (Figure 2a), while the in-plane orbitals of the metal→ligand back-donation have π symmetry (Figure 2b). The latter orbitals are denoted with the symbol $\pi_\parallel$ in order to distinguish them from the out-of-plane $\pi_\perp$ orbitals, which yield the metal←ligand π donation (Figure 2c) that may become important in alkyne complexes where the ligand serves as a four-electron donor. Finally there are the out-of-plane orbitals that yield metal→ligand back-donation (Figure 2d). The latter orbitals have δ

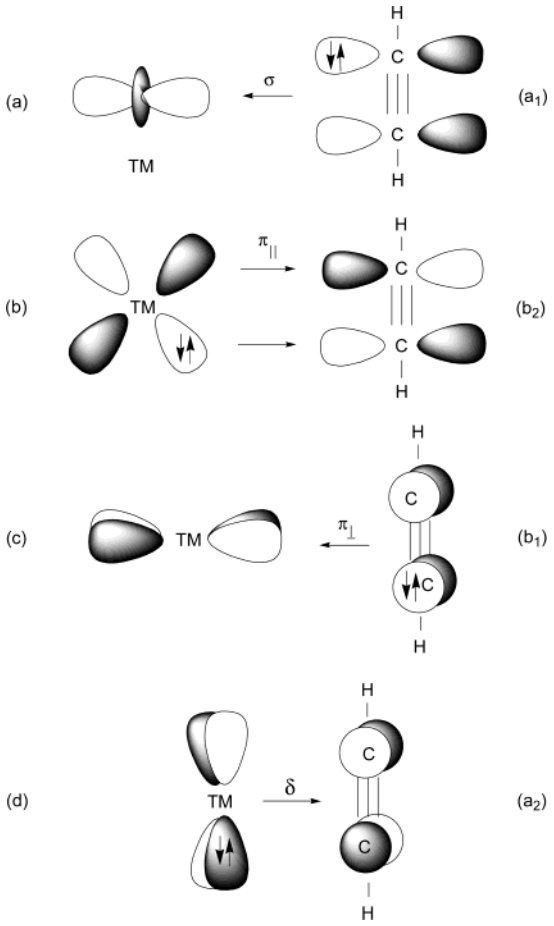

Figure 2. Schematic representation of the most important orbital interactions in TM−alkyne complexes: (a) ligand→metal in-plane σ donation; (b) metal→ligand in-plane $\pi_{||}$ back-donation; (c) ligand→metal out-of-plane $\pi_{\perp}$ donation; (d) metal→ligand δ donation. The symmetry assignments a_1, b_2, b_1, a_2 are given with respect to overall C_{2v} symmetry.

symmetry. They come from the mixing of the occupied d_{yz} AO of the metal and the vacant $\pi_{\perp}$* orbital of the ligand, where the symmetry assignment of the latter refers to the local symmetry of the free ligand.

The complexes $(PH_3)_2TM-C_2H_x$ and $(PMe_3)_2TM-C_2H_x$ have C_{2v} symmetry. Under C_{2v} symmetry, the four orbital interactions shown in Figure 2 have the symmetries $a_1(\sigma)$, $a_2(\delta)$, $b_1(\pi_{\perp})$, and $b_2(\pi_{||})$. The calculated values of ΔE_{orb} for orbitals having different symmetry give therefore a quantitative estimate of the strength of the interactions, which are schematically shown in Figure 2. The results in Tables 1 and 2 show that the $b_2(\pi_{||})$ interactions deliver the largest contribution to the ΔE_{orb} term. According to the EPA calculations, the TM→C_2H_x in-plane π back-donation yields between 64.9 and 78.5% of the total covalent bonding. The relative contribution of the TM←C_2H_x σ donation is much less. The values of the $a_1(\sigma)$ orbitals are between 18.2 and 34.4%. The percentage values of the ethyne complexes are always slightly larger for the $b_2(\pi_{||})$ contribution and smaller for the $a_1(\sigma)$ contribution compared with the ethene complexes, respectively. The contributions of the $a_2(\delta)$ and $b_1(\pi_{\perp})$ orbital interactions are very small even for the ethyne complexes, where the largest percentage value is found for the $(PH_3)_2TM$←$_2H_2$ $\pi_{\perp}$ donation (5.1%) (TM = Ni, Pt). The energy values show clearly that *the ethyne ligand in the complexes* $(PH_3)_2TM-C_2H_2$ *and* $(PMe_3)_2TM-C_2H_2$ *should be considered as a two-electron donor and not as a four-electron donor.*

The complexes (dpm)TM−C_2H_x and (dpe)TM−C_2H_x have C_s and C_2 symmetry, respectively. Therefore, only the interactions of orbitals having a′ and a″ symmetry in C_s and a and b in C_2 can be distinguished by the EPA calculations. The a′ orbital interactions of the complexes with C_s symmetry correspond to the $a_1(\sigma)$ and $b_1(\pi_{\perp})$ interactions of the complexes with C_{2v} symmetry, and the a″ interactions correspond to $a_2(\delta) + b_2(\pi_{||})$. On the contrary the a orbital interactions of the complexes with C_2 symmetry correspond to the $a_1(\sigma)$ and $a_2(\delta)$ interactions of the complexes with C_{2v} symmetry, and the b interactions correspond to $b_1(\pi_{\perp}) + b_2(\pi_{||})$.[60] The contributions of the $b_1(\pi_{\perp})$ and $a_2(\delta)$ orbital interactions in $(PH_3)_2TM-C_2H_2$ and $(PMe_3)_2TM-C_2H_2$ are rather small. They can also safely be assumed to be small in (dpm)-TM−C_2H_x and (dpe)TM−C_2H_x. Tables 3 and 4 give the calculated values for the a′(σ) and a″(π) orbital contributions in (dpm)TM−C_2H_x and for the a(σ) and b(π) orbital contributions in (dpe)TM−C_2H_x. The energy values of the a″(π) (and b(π)) orbitals are much larger than those of the a′(σ) (and a(σ)) orbitals. The comparison of the percentage contributions of the a′(σ) and a″(π) (C_s) and a(σ) and b(π) (C_2) orbital terms with comparison to the $a_1(\sigma)$, $b_1(\pi_{\perp})$, $a_2(\delta)$, and $b_2(\pi_{|})$ values, which are given in Tables 1 and 2, shows that the nature of the orbital interactions does not exhibit a large variation between the complexes with the monodentate and bidentate phosphane ligands.

The qualitative MO bonding model in Figure 2 suggests that all orbital interactions should yield a lengthening of the carbon−carbon bond of the π ligand. Figure 3 shows a diagram where the optimized C−C distances of the complexes $L_2TM-C_2H_4$ and $L_2TM-C_2H_2$ are plotted against the calculated ΔE_{orb} values. There is a nice correlation between the bond lengths and the orbital interactions, which quantitatively supports the DCD bonding model. A correlation of the bond strength given by the dissociation energies with the C−C bond lengths gives a very poor agreement.

The EPA results in Tables 1−4 show that the complexes with monodentate and bidentate ligands exhibit also a similar degree of covalent and electrostatic bonding between the metal and the π ligand. It follows that the nature of the $L_2TM-C_2H_x$ bonding does not change very much when L_2 comprises either a bidentate or two monodentate phosphane ligands. The main difference between the bonding in the two classes of

(59) (a) Hansen, S. M.; Volland, M. A. O.; Rominger, F.; Eisenträger, F.; Hofmann, P. *Angew. Chem.* **1999**, *111*, 1360; *Angew. Chem., Int. Ed.* **1999**, *38*, 1273. (b) Adlhart, C.; Volland, M. A. O.; Hofmann, P.; Chen, P. *Helv. Chim. Acta* **2000**, *83*, 3306. (c) Hofmann, P.; Volland, M. A. O.; Hansen, S. M.; Eisenträger, F.; Gross, J. H.; Stengel, K. *J. Organomet. Chem.* **2000**, *606*, 88. (d) Volland, M. A. O.; Hofmann, P. *Helv. Chim. Acta* **2001**, *84*, 3456. (e) Volland, M. A. O.; Straub, B. F.; Gruber, I.; Rominger, F.; Hofmann, P. *J. Organomet. Chem.* **2001**, *617−618*, 288. (f) Volland, M. A. O.; Adlhart, C.; Kiener, C. A.; Chen, P.; Hofmann, P. *Chem. Eur. J.* **2001**, *7*, 4621. (g) Urtel, H.; Bikzhanova, G. A.; Grotjahn, D. B.; Hofmann, P. *Organometallics* **2001**, *20*, 3938. (h) Urtel, H.; Meier, C.; Eisenträger, F.; Rominger, F.; Joschek, J. P.; Hofmann, P. *Angew. Chem.* **2001**, *113*, 803; *Angew. Chem., Int. Ed.* **2001**, *40*, 781.

(60) Note that there are no genuine orbitals which have σ, π, or δ symmetry in the complexes (dpe)TM−C_2H_x because there is no symmetry plane in the point group C_2. However, the local mirror symmetry of the C_2H_x ligands is nearly undisturbed by the dpe ligand, and thus, the orbital interactions can safely be divided into σ and π contributions.

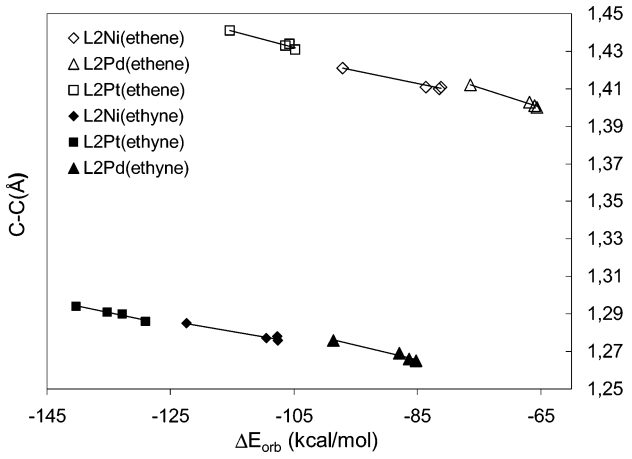

Figure 3. Plot of the optimized C−C distances of $L_2TM-C_2H_x$ and the orbital interaction term ΔE_{orb}.

compounds comes from the significantly larger deformation energy of the metal fragment with two monodentate phosphane ligands $(PR_3)_2TM$ compared with bidentate metal fragments such as (dpm)TM and (dpe)TM, which yields a higher $L_2TM-C_2H_x$ bond dissocation energy for the latter species. This finding could be helpful for the interpretation and understanding of the peculiar chemistry of transition metal complexes with ligands such as bis(di-*tert*-butylphosphino)ethane (dtbpe) and bis(di-*tert*-butylphosphino)methane (dtbpm), which have been found useful in homogeneous catalysis.[59]

Summary

The results of the theoretical work can be summarized as follows.

The DFT calculations predict that the ethene and ethyne ligands of the complexes $L_2TM-C_2H_x$ are more strongly bonded to the metal when L_2 is a bidentate phosphane ligand like dpm or dpe compared with monodentate ligands $(PH_3)_2$ and $(PMe_3)_2$. The energy-partitioning analysis of the bonding situation reveals that the reason for the stronger bonds of (dpm)TM−C_2H_x and (dpe)TM−C_2H_x is the smaller preparation energy of (dpm)TM and (dpe)TM that is necessary to deform the metal fragments from the equilibrium geometry to the geometry in the complex. The EPA results show that the nature of the $L_2TM-C_2H_x$ bonding does not significantly change when L_2 consists of a bidentate or two monodentate ligands. The metal−carbon bonds have a higher electrostatic (54.1−62.3%) than covalent (37.7−45.9%) character. The covalent bonding in the ethyne and ethene complexes comes mainly from the TM$\rightarrow_2H_x$ in-plane π back-donation, while the relative contribution of the TM$\leftarrow C_2H_x$ σ donation is much smaller. The contributions of the out-of-plane $a_2(\delta)$ and $b_1(\pi_\perp)$ orbital interactions are very small even for the ethyne compounds. The bonding analysis suggests that the ethyne ligand in the complexes $(PH_3)_2TM-C_2H_2$ and $(PMe_3)_2TM-C_2H_2$ should be considered as a two-electron donor and not as a four-electron donor.

Acknowledgment. This work was supported by the Deutsche Forschungsgemeinschaft and by the Fonds der Chemischen Industrie. C.M. thanks the Deutscher Akademischer Austauschdienst for a research fellowship. Excellent service by the Hochschulrechenzentrum of the Philipps-Universität Marburg is gratefully acknowledged.

Supporting Information Available: Tables with the coordinates of the optimized structures at BP86/TZP. This material is available free of charge via the Internet at http://pubs.acs.org.

OM0301637